Acta Crystallographica Section D
Biological Crystallography
ISSN 0907-4449

Structure of a novel α-amylase AmyB from *Thermotoga neapolitana* that produces maltose from the nonreducing end of polysaccharides

So-Young Jun,[a] Jin-Sik Kim,[a] Kyoung-Hwa Choi,[b] Jaeho Cha[b] and Nam-Chul Ha[a]*

[a]Department of Manufacturing Pharmacy and Research Institute for Drug Development, Pusan National University, Busan 609-735, Republic of Korea, and [b]Department of Microbiology, College of Natural Sciences, Pusan National University, Busan 609-735, Republic of Korea

Correspondence e-mail: hnc@pusan.ac.kr

Received 29 August 2012
Accepted 30 November 2012

PDB Reference: AmyB, 4gkl

An intracellular α-amylase, AmyB, has been cloned from the hyperthermophilic bacterium *Thermotoga neapolitana*. AmyB belongs to glycoside hydrolase family 13 and liberates maltose from diverse substrates, including starch, amylose, amylopectin and glycogen. The final product of AmyB is similar to that of typical maltogenic amylases, but AmyB cleaves maltose units from the nonreducing end, which is a unique property of this α-amylase. In this study, the crystal structure of AmyB from *T. neapolitana* has been determined at 2.4 Å resolution, revealing that the monomeric AmyB comprises domains A, B and C like other α-amylases, but with structural variations. In the structure, a wider active site and a putative extra sugar-binding site at the top of the active site were found. Subsequent biochemical results suggest that the extra sugar-binding site is suitable for recognizing the nonreducing end of the substrates, explaining the unique activity of this enzyme. These findings provide a structural basis for the ability of an α-amylase that has the common α-amylase structure to show a diverse substrate specificity.

1. Introduction

Thermotoga neapolitana is an anaerobic fermentative heterotrophic marine hyperthermophilic bacterium that was isolated from heated sea floors (Windberger *et al.*, 1989). Members of the genus *Thermotoga* have been investigated as sources of hyperthermophilic mannanases, xylanases and amylases (Saul *et al.*, 1995; Ballschmiter *et al.*, 2006; Parker *et al.*, 2001) since they have a very large number of genes for carbohydrate-active enzymes. *T. neapolitana* can degrade a wide variety of α-linked and β-linked glucans through an anaerobic fermentative metabolism (Bibel *et al.*, 1998; Bok *et al.*, 1998; Conners *et al.*, 2005; Miller *et al.*, 2001; Bronnenmeier *et al.*, 1995; Chhabra *et al.*, 2001, 2002, 2003; Duffaud *et al.*, 1997). Recently, an intracellular enzyme, AmyB, was cloned from *T. neapolitana* and characterized as a unique type of α-amylase (α-D-1,4-glucan-4-gluconohydrolase; EC 3.2.1.1; Park *et al.*, 2010).

Most α-amylases are assigned to the glycoside hydrolase 13 (GH13) family, which are multidomain $(\alpha/\beta)_8$-barrel enzymes that show a large variation in the structural motif to provide an array of substrate specificities (Svensson, 1994). Numerous α-amylases have been cloned and characterized structurally, providing insight into the relationship between structure and substrate specificity. Typical α-amylases, including *Aspergillus oryzae* TAKA α-amylase (Matsuura *et al.*, 1979, 1980), consist of three conserved domains named A, B and C. Domain A

exhibits a TIM-barrel structure that makes up the core part of the molecule, and domain B is an irregular β-strand structure that is inserted in the middle of the TIM barrel. Domain C contains β-strands that make up a Greek-key motif and is connected to the C-terminal region of the TIM barrel (Svensson, 1994). Domains A and B are known to be responsible for the catalytic activity of α-amylases, while the function of domain C remains to be elucidated.

AmyB, a member of the GH13 family, can hydrolyze soluble starch, amylose, amylopectin and glycogen, which are bulky or highly branched polysaccharides (Park *et al.*, 2010). AmyB is an exo-acting α-amylase that mostly liberates maltose from the nonreducing end of substrates. The only activity of AmyB is α-D-1,4-glucosidic bond cleavage; it does not share catalytic characteristics with cyclodextrin-hydrolyzing enzymes, which catalyze the hydrolysis of cyclodextrin (CD), pullulan and acarbose (Park *et al.*, 2010).

The final product of AmyB is most similar to those of the maltogenic amylases (EC 3.2.1.133) among GH13 α-amylases (Park *et al.*, 2010). However, AmyB is distinct from typical maltogenic amylases in many aspects. Typical maltogenic amylases produce maltose from the reducing end of the substrates by transglycosylase activity (Park *et al.*, 2000) and also possess dual activity for α-D-1,4- and α-D-1,6-glucosidic bond cleavage, thus differing from the classic α-amylases in the GH13 family (MacGregor *et al.*, 2001). Unlike AmyB, maltogenic amylases can cleave CD, pullulan and acarbose, sharing this activity with CD-hydrolyzing enzymes (Park *et al.*, 2000). Thus, AmyB is a new type of exo-acting α-amylase that possesses distinct characteristics that distinguish it from typical α-amylases and typical bacterial maltogenic endo-acting amylases (Park *et al.*, 2010).

In this study, we determined the crystal structure of AmyB at 2.4 Å resolution and characterized the putative maltose-binding site which accounts for the substrate specificity and catalytic properties of AmyB.

2. Materials and methods

2.1. Cloning and expression

A DNA fragment encoding full-length AmyB (residues 1–422) was amplified from the genomic DNA of *T. neapolitana* using the polymerase chain reaction. The DNA fragment was inserted into the *Kpn*I and *Eco*RI sites of pET29b(+) (Novagen). The resulting protein contained an uncleavable hexahistidine tag at the C-terminus.

2.2. Purification

The recombinant AmyB protein was expressed in *Escherichia coli* strain BL21 (DE3). Protein expression was induced by the addition of 0.2 m*M* isopropyl β-D-1-thiogalactopyranoside (IPTG). The culture was harvested by centrifugation. The cells were resuspended in 20 m*M* Tris buffer pH 8.0 and disrupted by sonication. The crude cell extract was centrifuged at 12 000*g* (20 min, 277 K) to remove cell debris. The supernatant was then incubated at 353 K for 30 min to denature thermolabile host proteins and centrifuged again at 12 000*g* (30 min, 277 K) to remove denatured protein from the extract. The resulting supernatant was dialyzed against 20 m*M* sodium phosphate pH 6.5 at 277 K overnight and subjected to cation-exchange chromatography using a HiTrap SP HP column (GE Healthcare, USA) equilibrated with the same buffer. Elution was carried out with a 0–1.0 *M* NaCl gradient in the same buffer in 15 column volumes at a flow rate of 1.0 ml min^{-1}. The collected fractions containing the AmyB protein were pooled, concentrated and separated on a HiLoad Superdex 200 gel-filtration column (GE Healthcare, USA) pre-equilibrated with 20 m*M* Tris buffer pH 8.0 containing 150 m*M* NaCl and 2 m*M* β-mercaptoethanol. The purified protein was concentrated to 20 mg ml^{-1} using Ultra centrifugal filter devices (Millipore, Eschborn, Germany).

2.3. Site-directed mutagenesis

The D135A and D169N mutations were introduced into the cloned wild-type AmyB gene by two subsequent PCR reactions (Landt *et al.*, 1990). The correctness of the mutagenized genes was confirmed by sequencing the genes. The mutant proteins were purified using the same method as used for the wild-type enzyme.

2.4. Enzyme-activity assays

2.4.1. α-Amylase assays using maltotriose as a substrate. To examine the hydrolytic patterns of AmyB, purified AmyB (40 ng) was incubated with 500 µl of 0.25, 0.5, 1 or 2%(*w*/*v*) maltotriose in 20 m*M* sodium phosphate buffer pH 6.5. Each reaction was incubated at 348 K for 12 h and subsequently immediately placed in an ice–water bath to stop the reaction. The resulting reaction products were analyzed by thin-layer chromatography (TLC) on Whatman K5F silica-gel plates (Whatman, Maidstone, England) with 1-butanol/ethanol/H_2O [5:5:3(*v*:*v*:*v*)] as the solvent system. After irrigating twice, the TLC plate was dried and visualized by dipping it into a solution consisting of 0.3%(*w*/*v*) *N*-(1-naphthyl)-ethylenediamine and 5%(*v*/*v*) H_2SO_4 in methanol and then heating for 5 min at 393 K (Robyt & Mukerjea, 1994).

2.4.2. α-Glucosidase activity using *p*-nitrophenyl glucopyranoside or *p*-nitrophenyl maltopyranoside as a substrate. α-Glucosidase activity was measured using a modification of a previously reported method (Kim *et al.*, 2005). A reaction mixture (100 µl) consisting of 125 ng enzyme and 5 m*M* *p*-nitrophenyl glucopyranoside (pNPG) or *p*-nitrophenyl maltopyronoside ($pNPG_2$) in 20 m*M* sodium phosphate buffer pH 6.5 was incubated at 348 K for 2.5 min or 16 h. The reaction was stopped by the addition of 100 µl 1 *M* Na_2CO_3. The α-glucosidase activity was determined by measuring the release of *p*-nitrophenol from pNPG or $pNPG_2$ at 405 nm using a UV–Vis spectrophotometer.

2.5. Crystallization and data collection

The initial crystallization of AmyB was performed by the sitting-drop vapour-diffusion method using commercially available screening solutions (Hampton Research, USA).

Table 1
Data-collection and refinement statistics.

Value in parentheses are for the highest resolution shell.

Data set	
Source	Photon Factory AR
Wavelength (Å)	1.0000
Temperature (K)	100
Resolution limits (Å)	20–2.40 (2.44–2.40)
Space group	$P2_1$
Unit-cell parameters (Å)	a = 66.8, b = 74.5, c = 108.9
Unique reflections	37665
Multiplicity	3.6 (2.3)
R_{merge} (%)	9.9 (22.2)
Completeness (%)	94.1 (86.1)
$\langle I/\sigma(I)\rangle$	14.8 (3.2)
Refinement	
Resolution range (Å)	20–2.40
R factor (%)	19.7
R_{free}† (%)	26.3
Average B value (Å^2)	28.4
R.m.s.d. for bonds (Å)	0.008
R.m.s.d. for angles (°)	1.278
No. of protein atoms	7021
No. of water atoms	244
Ramachandran plot (%)	
Most favoured	87.9
Additionally allowed	11.2
Generously allowed	0.7
Disallowed	0.3
PDB code	4gkl

† R_{free} was calculated with 5% of the data set.

Crystals with a thick plate shape were grown at 287 K by the hanging-drop vapour-diffusion method. Equal volumes (about 1 µl) of 15 mg ml^{-1} protein solution and a reservoir solution consisting of 0.1 *M* sodium acetate pH 4.6, 2.0 *M* sodium formate were mixed. For cryoprotection, the crystals were briefly soaked in a solution consisting of 0.1 *M* sodium acetate pH 4.6 and saturated sodium formate. X-ray diffraction data were collected from flash-cooled crystals using an ADSC CCD detector on beamline NW3A of Photon Factory AR (Japan) at 100 K. Typical data sets consisted of 360 frames with 1° rotation and 2 s exposure time per image. The diffraction data sets were processed and scaled to 2.4 Å resolution using the *HKL*-2000 package (Otwinowski & Minor, 1997), which revealed a primitive monoclinic lattice with unit-cell parameters a = 66.9, b = 74.4, c = 108.9 Å, α = 90, β = 107.8, γ = 90°. Systemic absences along the z axis revealed the space group to be $P2_1$. X-ray data statistics are summarized in Table 1.

2.6. Structural determination and refinement

The initial phases were determined using the *MOLREP* molecular-replacement package (Vagin & Teplyakov, 2010) with the coordinates of α-amylase from *Lactobacillus plantarum* (PDB entry 3dhu; New York SGX Research Center for Structural Genomics, unpublished work) as a search model. Model building was performed using *Coot* (Emsley & Cowtan, 2004) and refinement was carried out using *phenix.refine* (Adams *et al.*, 2002). A random set of 5% of reflections was excluded from refinement for cross-validation of the refinement strategy. Owing to missing electron density, residues 132 and 133 are missing from the model. Water molecules were assigned automatically for peaks of >2σ in $F_o - F_c$ difference maps by cycling *phenix.refine* refinement and were verified by manual inspection. The quality of the model was checked using *PROCHECK* (Laskowski *et al.*, 1996). Most residues were in the favoured region of the Ramachandran plot, except for Arg412, which was located in a region of weak electron density. Refinement statistics are summarized in Table 1. The coordinates and structure factors have been deposited in the Protein Data Bank (PDB entry 4gkl). Figures were generated using *PyMOL* (DeLano, 2002).

2.7. Preparation of acarbose-coupled aminohexyl-Sepharose resin

Acarbose-coupled aminohexyl-Sepharose resin was prepared using a previously described method (Clarke & Svensson, 1984). In brief, acarbose [2%(*w*/*v*)] was activated with cyanogen bromide in 20 m*M* phosphate buffer pH 10.5 for 2 h and coupled to aminohexyl-Sepharose in 0.2 *M* sodium borate pH 8.7 overnight at 277 K.

3. Results and discussion

3.1. Structure determination

The crystals of AmyB belonged to the monoclinic space group $P2_1$. The Matthews coefficient (V_M = 2.71 Å^3 Da^{-1}) suggested the presence of two molecules in the asymmetric unit and a corresponding solvent content of 54.7%. The crystal structure of AmyB was determined by means of molecular replacement using residues 30–330 of a putative α-amylase from *L. plantarum* (PDB entry 3dhu) as a search model. The search model was chosen because it showed the highest primary sequence similarity to AmyB among the available structures. However, only the N-terminal part was used in molecular replacement since the C-terminal part showed poor sequence similarity. The rotation and translation functions gave prominent solutions, producing a high-quality electron-density map for the region of AmyB corresponding to the search model. After several rounds of refinement, the electron-density map for the remaining region became traceable. The final model of AmyB at 2.4 Å resolution encompassed all N- and C-terminal residues but lacked two residues (132 and 133) that did not display any visible electron density. The asymmetric unit in the crystal contained two molecules that were almost identical (r.m.s.d. of 0.286 Å between 396 C^α atoms). The structure was refined to a free R value of 26.1% with good stereochemistry (Table 1).

3.2. Overall structure

The overall structure of AmyB can be separated into two major parts: an N-terminal domain (domains A and B; residues 1–334) and a C-terminal domain (domain C; residues 335–422) (Fig. 1*a*). Examination of the N-terminal domain revealed that it contains the two conserved domains found in typical α-amylases (named domains A and B). Domain A (residues 1–101 and 141–334) forms the central part of the N-terminal domain and makes up a classical $(\alpha/\beta)_8$ TIM-barrel

structure. Domain B is small (residues 102–140) and protrudes from the larger domain A by interrupting between the third strand and third α-helix of the $(\alpha/\beta)_8$ TIM-barrel structure of domain A. Domain B is composed of two short α-helices and two short β-strands (Fig. 1) and shows variation in amino-acid sequence and structure from other α-amylases (Fig. 2). The disordered region in the final model is found in domain B, indicating high flexibility of these residues. The C-terminal domain is composed of eight β-strands in a Greek-key motif and is referred to as domain C in the α-amylases (Fig. 1*a*).

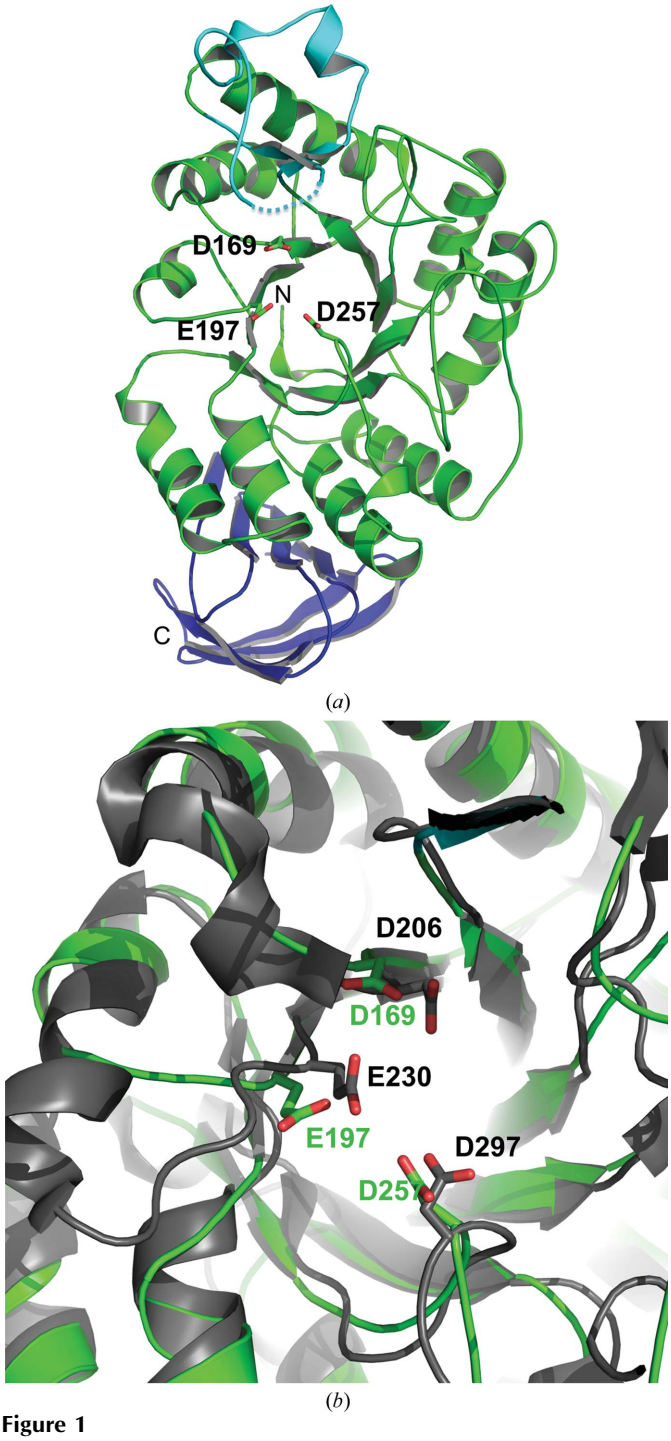

Figure 1
Overall structure of AmyB. (*a*) Ribbon representation of AmyB. Domains A, B and C are represented in green, cyan and blue, respectively. The three catalytic residues (Asp169, Glu197 and Asp257) that are strictly conserved in the α-amylase superfamily are shown in stick representation. (*b*) Superposition of the catalytic residues of AmyB with those of TAKA α-amylase. AmyB is shown in green and TAKA α-amylase in grey.

The two molecules in the asymmetric unit only exhibit slight contacts in the crystal packing, indicating that AmyB functions as a monomer. This observation is consistent with a previous result indicating that the protein is monomeric in solution (Park *et al.*, 2010).

3.3. Conserved catalytic residues

Multiple protein sequence alignment and biochemical and structural studies of GH13-family starch hydrolases revealed the invariant catalytic residues Asp206, Glu230 and Asp297 (TAKA α-amylase numbering; Janecek *et al.*, 1997; Svensson, 1994). The deprotonated Asp206 makes a nucleophilic attack on the substrate and the protonated Glu230 donates a proton to the leaving group. Asp297 makes a hydrogen bond to Glu230, which may play a role in raising the pK_a of Glu230 (McCarter & Withers, 1994). Sequence alignment and structural superposition of AmyB with TAKA α-amylase confirms the presence of the conserved catalytic residues Asp169, Glu197 and Asp257 (in AmyB numbering), which are located at the centre of the TIM barrel (Figs. 1*b* and 2). This suggests that AmyB shares its catalytic mechanism with TAKA α-amylase.

3.4. Structural comparison with *L. plantarum* α-amylase

Although the structure of *L. plantarum* α-amylase has been deposited, the structure and biochemical characteristics of this protein have not been reported. Since α-amylase from *L. plantarum* shows a high degree of sequence identity (42%) to AmyB, the structure of *L. plantarum* α-amylase was used as a search model in molecular replacement. When AmyB was superimposed with α-amylase from *L. plantarum*, the overall structure of AmyB matched that of *L. plantarum* α-amylase well (r.m.s.d. of 1.172 Å between 289 C^{α} atoms; Fig. 3*a*, left). However, they differ in the α-helix between the fifth and sixth β-strands of the TIM barrel of domain A. *L. plantarum* α-amylase has an long insertion (16 amino acids; Fig. 2, red box) compared with AmyB that is located on the right side of the active-site cleft. As shown in Fig. 3(*a*), the additional region of *L. plantarum* α-amylase forms an α-helix and loops and lines the active-site pocket. Owing to the lack of this insertion in AmyB, AmyB has a wider active-site cleft compared with *L. plantarum* α-amylase (Fig. 3*b*). This wide active-site cleft might be involved in the catalytic activity of AmyB towards bulky or branched polysaccharides.

Domain C of AmyB (residues 335–422) and domain C of *L. plantarum* α-amylase do not share significant sequence similarity. Although domain C of AmyB and domain C of *L. plantarum* α-amylase both have the common structural motif known as a Greek key, many differences are present in the detailed structure and in the relative location of domain C with respect to domain A (Fig. 3*a*). Even though most

α-amylases contain domain C, its precise function remains unclear (Svensson, 1994). Thus, further studies on domain C are required in order to determine the importance of the structural variation of domain C of AmyB.

3.5. Structural comparison with TAKA α-amylase

TAKA α-amylase is a typical endo-acting α-amylase and displays high sequence similarity to AmyB (sequence similarity of 40%). Although AmyB exhibits a similar structure to TAKA α-amylase when superposed (r.m.s.d. of 2.32 Å between 234 C^{α} atoms), many structural differences are displayed, particularly in domains B and C. Domain B of TAKA α-amylase has an elongated loop compared with AmyB and *L. plantarum* α-amylase (Fig. 2) that is stabilized by a disulfide bridge. The elongated loop of TAKA α-amylase domain B lines the right side of the active-site cleft like the long insertion in domain A of *L. plantarum* α-amylase (Fig. 3*a*, right).

The relative position of domain C in AmyB is significantly different from that of TAKA α-amylase despite having the same overall fold (Fig. 3*a*, right).

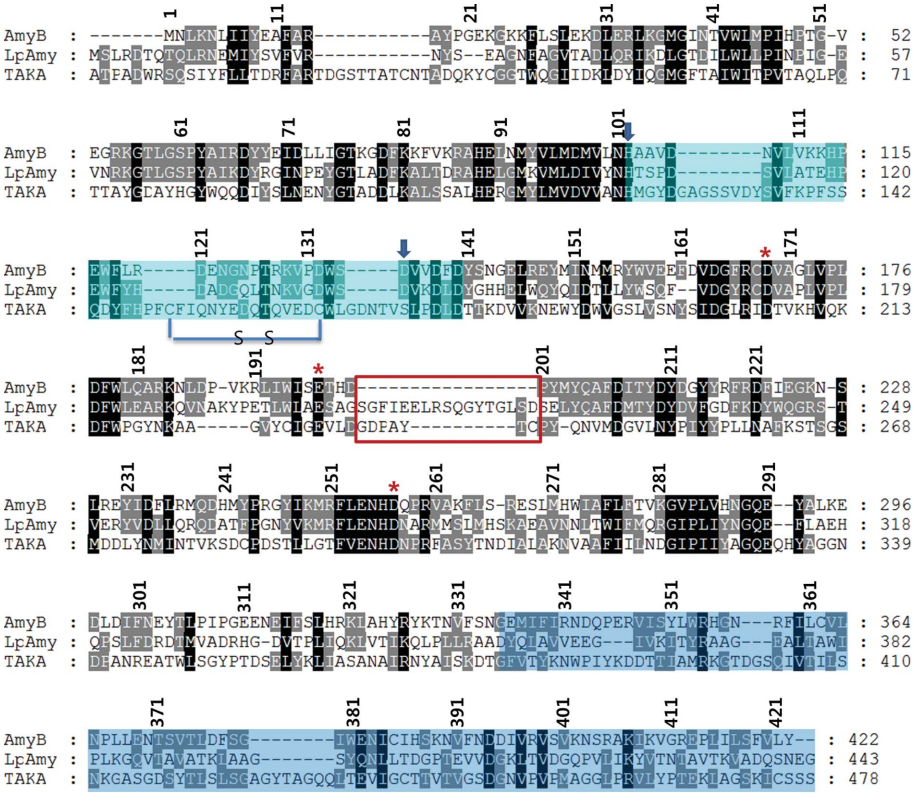

Figure 2
Sequence alignment of the *T. neapolitana* α-amylase AmyB (AmyB; ACF75909), *L. plantarum* α-amylase (LpAmy; PDB entry 3dhu) and TAKA α-amylase (TAKA; BAA00336). The sequences of the three enzymes were aligned using *ClustalW* and then modified based on the structures (Thompson *et al.*, 1997). Domain B is shaded in cyan, domain C is shaded in blue and domain A is not shaded. The red asterisks above the sequence indicate the essential catalytic residues conserved in the α-amylase enzymes. The residue number of AmyB is indicated every ten residues above the sequence. The red box indicates the insertion in *L. plantarum* α-amylase. The arrows indicate the residues that might be involved in the 'nonreducing end binding site'.

3.6. Comparison with dimeric maltogenic amylases

The exo-acting maltogenic amylases harbour multiple enzymatic activities that are distinct from other α-amylases (Kim *et al.*, 1992). The crystal structure of maltogenic amylase from *Thermus* (ThMA) revealed that formation of the dimer is mediated by the novel additional N-terminal domain (Kim, Kim *et al.*, 1999). An extra sugar-binding site was found in ThMA near the substrate-binding site. The sugar-binding site is lined by the N-terminal domain of the other subunit of the ThMA dimer. The glucose molecule in the extra sugar-binding site could serve as an acceptor molecule that attacks the substrate intermediate using its transglycosylation activity, which may account for the maltose-producing nature of the enzyme (Kim, Cha *et al.*, 1999).

Like the maltogenic amylases, AmyB produces maltose as a product (Park *et al.*, 2010). However, it differs from the typical maltogenic amylases in many aspects. AmyB is monomeric and does not have the additional N-terminal domain that is responsible for the dimerization of maltogenic amylases (Park *et al.*, 2010). Another striking difference is that AmyB releases maltose from the nonreducing end of oligosaccharides, while the typical maltogenic amylases cleave the glucose unit from the reducing end of the substrate. Furthermore, AmyB does not exhibit transglycosylation activity (Park *et al.*, 2010). Its lack of the N-terminal domain and its dimeric nature indicate that AmyB does not harbour the corresponding extra sugar-binding site. Moreover, the conserved Glu332 of ThMA that is crucial for transglycosylation activity in the extra sugar-binding site is replaced by a leucine in AmyB (Fig. 3*c*). Thus, these findings indicate that AmyB is able to produce maltose like ThMA and further suggest that AmyB produces maltose using a different mechanism compared with the typical maltogenic amylases.

3.7. Nonreducing end sugar-binding site

An extra space was observed at the top of the active-site cleft of AmyB (Fig. 3*b*). This space is largely lined by Asp135 and His103 from domain B and could accommodate a monosaccharide. A maltotriose molecule consisting of three glucose molecules was docked into the AmyB active site using the TAKA α-amylase in complex with maltose (PDB entry 2gvy; Vujičić-Žagar & Dijkstra, 2006) as a reference. In the docking model, a maltotriose molecule fitted nicely into the active-site cleft, in which the nonreducing end of the

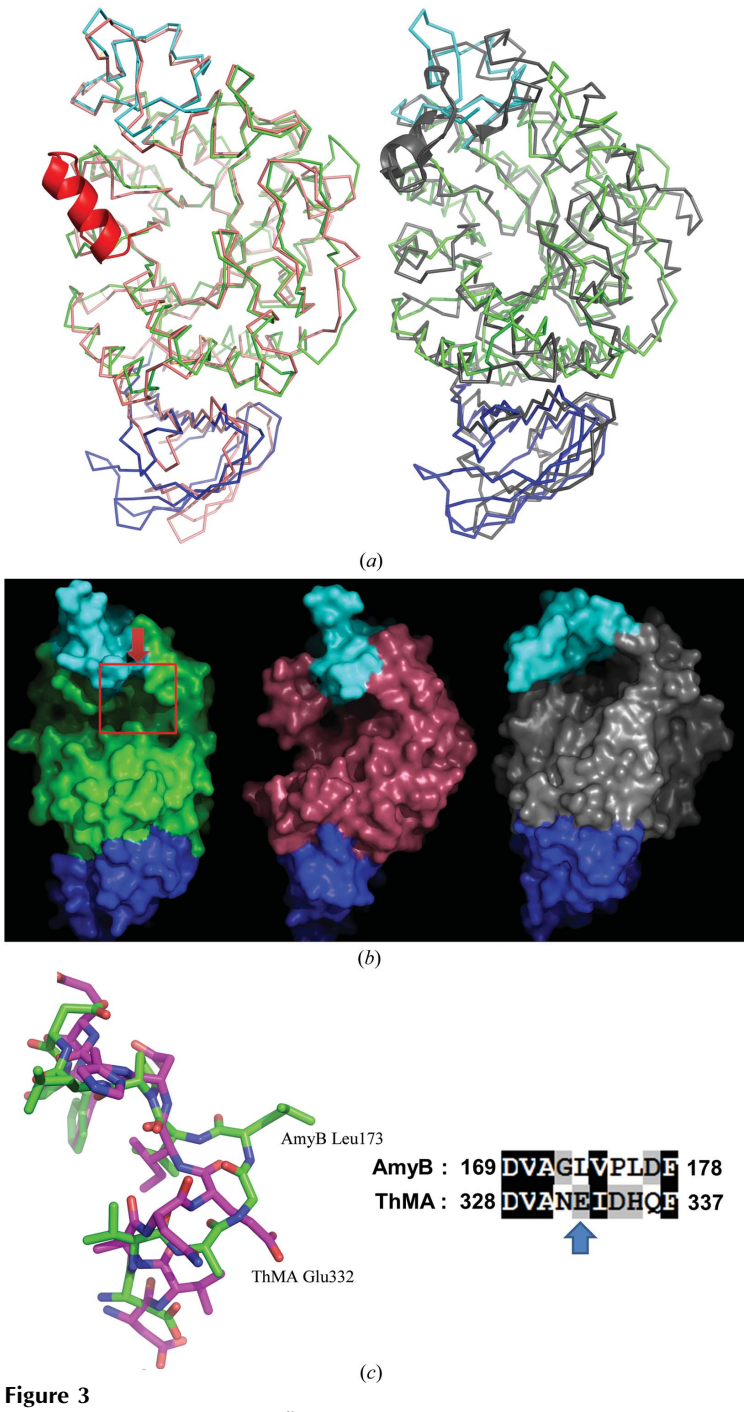

Figure 3
Structural comparison. (*a*) C^{α} representations of AmyB superposed with *L. plantarum* α-amylase (left) and TAKA α-amylase (right). Domains A, B and C of AmyB are coloured green, cyan and blue, respectively, *L. plantarum* α-amylase is coloured pale red and TAKA α-amylase is coloured grey. To highlight the insertion in domain A of *L. plantarum* α-amylase, the corresponding region is shown as a cartoon representation, as is the elongated loop in domain B of TAKA α-amylase. (*b*) Surface representations of AmyB (left), *L. plantarum* α-amylase (centre) and TAKA α-amylase (right) in the same orientation as in Fig. 1(*a*). Domain A is coloured differently (AmyB, green; *L. plantarum* α-amylase, pale red; TAKA α-amylase, grey). Domain B is coloured cyan and domain C is coloured blue. The red box in the left panel is enlarged in Fig. 4(*a*). The red arrow indicates the nonreducing end recognition site. (*c*) Structural superposition and sequence alignment of AmyB (green) with *Thermus* maltogenic amylase (ThMA; magenta) around the extra sugar-binding site of ThMA. The arrow indicates Glu332 of ThMA, which is strictly conserved among typical maltogenic amylase family members (Kim, Cha *et al.*, 1999).

maltotriose was docked into the extra space (Fig. 4*a*). Thus, the space is referred to as the 'nonreducing end sugar-binding site' in this study. We hypothesized that the nonreducing end sugar-binding site recognizes the nonreducing end monosaccharide of the substrate oligosaccharide and is important in the catalytic activity.

According to this hypothesis, the monosaccharide at the nonreducing end should be important in recognition of the substrate. Acarbose is a pseudotetrasaccharide that has an acarviosin moiety at the nonreducing end of maltose and an intact maltose unit at the reducing end. Acarbose is known to inhibit α-amylases through competitive binding to the active site. It has been reported that unlike typical maltogenic amylases, AmyB cannot cleave acarbose (Park *et al.*, 2010). In this study, we tested the possibility that acarbose might act as an inhibitor of AmyB by binding to the active site. As shown in Fig. 4(*b*), acarbose did not inhibit the α-amylase activity of AmyB when maltotriose was used as a substrate. To further examine the binding ability of acarbose to AmyB, acarbose-coupled aminohexyl-Sepharose resin was prepared and incubated with wild-type and mutant AmyB proteins. As a control, α-amylase from *Bacillus licheniformis*, which binds to acarbose (Brzozowski *et al.*, 2000), was used in the binding assay. As shown in Fig. 4(*c*), AmyB did not bind to the acarbose-coupled resin, unlike α-amylase from *B. licheniformis*. These results indicate that the binding affinity of acarbose to AmyB is very low, probably owing to the altered nonreducing end region, suggesting that the sugar moiety at the nonreducing end is important in binding to the active site of AmyB.

3.8. Functional importance of the nonreducing end sugar-binding site

To determine whether the nonreducing end binding site is involved in substrate recognition, we generated an AmyB variant (D135A) which harbours a mutation in the nonreducing end sugar-binding site. We measured the enzymatic activity using an ideal substrate, maltotriose. The wild-type enzyme efficiently cleaved the substrate, whereas the D135A mutation abolished the activity even at a high concentration of substrate (Fig. 4*a*). This result indicates that Asp135 plays an important role in the activity of AmyB.

Next, we examined whether Asp135 is directly involved in the catalytic process using a very short substrate, *p*-nitrophenyl glucopyranoside (pNPG), which contains only one glucose unit and a colouring moiety that is attached to the reducing end of the glucose. Although pNPG is a poor substrate for AmyB, prolonged incubation (16 h) with wild-type AmyB showed a measurable activity (Fig. 5*b*). With other α-amylases enzymatic activity was readily observed

within 30 min using a similar amount of enzyme (Kim *et al.*, 2005). The D135A mutant protein exhibited a comparable activity (~40%) to the wild-type enzyme in this pNPG-based assay, while mutation of the catalytic residue (D169N) completely abolished the activity (Fig. 5*b*). This result indicates that Asp135 does not function as a catalytic residue that is directly involved the catalytic mechanism.

For comparison with pNPG, *p*-nitrophenyl maltopyranoside ($pNPG_2$), a pNPG derivative, was used in an AmyB activity assay. As the colouring moiety is attached to the reducing end of the maltose, $pNPG_2$ has an unmodified nonreducing end. When $pNPG_2$ was docked into the active-site region of the AmyB crystal structure, the nonreducing end sugar was positioned at the nonreducing end binding site (+2 site). As expected, $pNPG_2$ was rapidly cleaved by the wild-type AmyB protein within 2.5 min, demonstrating that $pNPG_2$ is an excellent substrate, unlike pNPG (Fig. 5*c*). However, D135A mutant AmyB exhibited a very low activity (less than 3%) towards $pNPG_2$ compared with wild-type AmyB. These results show that AmyB strictly requires the intact nonreducing end binding site when cleaving $pNPG_2$, which can produce a maltose unit as a reaction product. Our results also confirm that the reducing end part of the substrate is not important for AmyB activity, considering the modified reducing end of the $pNPG_2$.

Combined with the biochemical results, our docked structure in which the nonreducing end binding site is responsible for the recognition of the nonreducing end of the substrate at the +2 site, as depicted in Fig. 5(*d*), is highly probable. This mechanism could account for the liberation of maltose units from the nonreducing end of substrates by AmyB. Furthermore, the mechanism can also explain the inactivity of AmyB towards CDs, which lack a nonreducing end.

4. Conclusion

We have crystallized and solved the structure of the α-amylase AmyB from *T. neapolitana*. AmyB liberates maltose from the nonreducing end of the substrate, which distinguishes it from other α-amylases. The crystal structure revealed that AmyB has a wider active site and an extra space at the top of the active site. In particular, we provide evidence that the extra space recognizes the nonreducing end of the substrate, accounting for the unique catalytic activity of AmyB. Our findings provide a structural basis for the ability of an α-amylase that has a common α-amylase structure to show diverse substrate specificity.

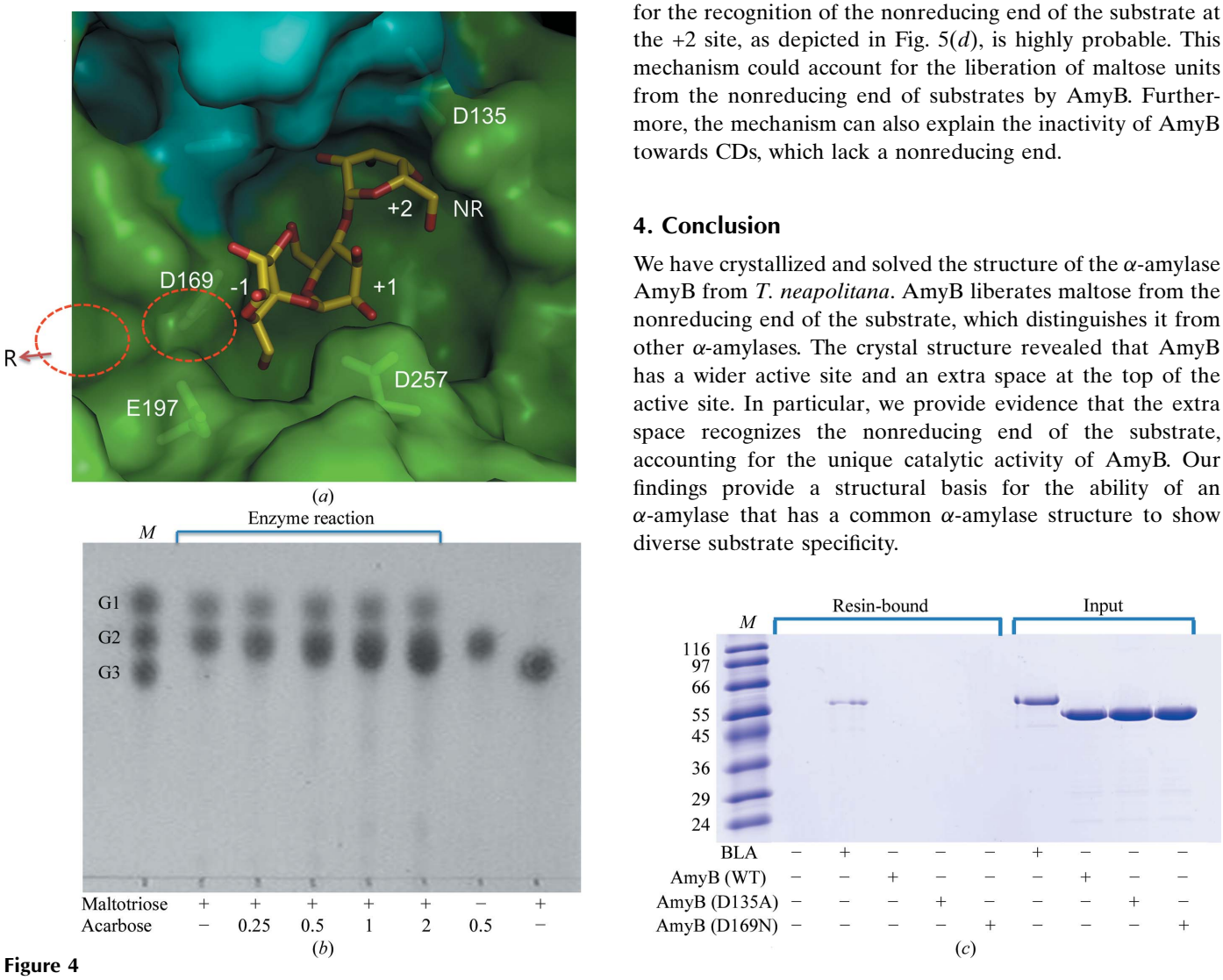

Figure 4
Substrate recognition of AmyB. (*a*) Modelling of maltotriose in the active site of AmyB (see the red box in Fig. 3*b*, left). A surface representation of the active-site pocket is shown with a hypothetical maltotriose molecule modelled in the active site. The nonreducing end of the sugar (NR) is fitted in the small pocket near Asp135. The extended region of the sugar is drawn as red circles. (*b*) Acarbose does not inhibit the α-amylase activity of AmyB in the α-amylase assay using maltotriose as a substrate. AmyB (40 ng) was incubated with 0.5% maltotriose and increasing concentrations of acarbose (0.25, 0.5, 1 and 2%) at 348 K for 12 h (enzyme reaction) and then subjected to TLC analysis. In the marker lane (*M*), G1, G2 and G3 indicate glucose, maltose and maltotriose, respectively. (*c*) Acarbose does not bind to AmyB. Wild-type or mutant AmyB proteins (D135A and D169N) or α-amylase from *B. licheniformis* (BLA; Sigma; 'Input'; 0.1 mg) was incubated with acarbose-coupled aminohexyl-Sepharose resin (20 µl) in 0.1 *M* sodium acetate buffer pH 4.3 containing 0.5 *M* sodium chloride. After washing, each resin was applied to SDS–PAGE to examine the amount of protein bound ('Resin-bound'). The gel was stained using Coomassie Blue. See the main text for the D135A and D169N mutants. Protein size standards are shown in lane *M* and are labelled in kDa.

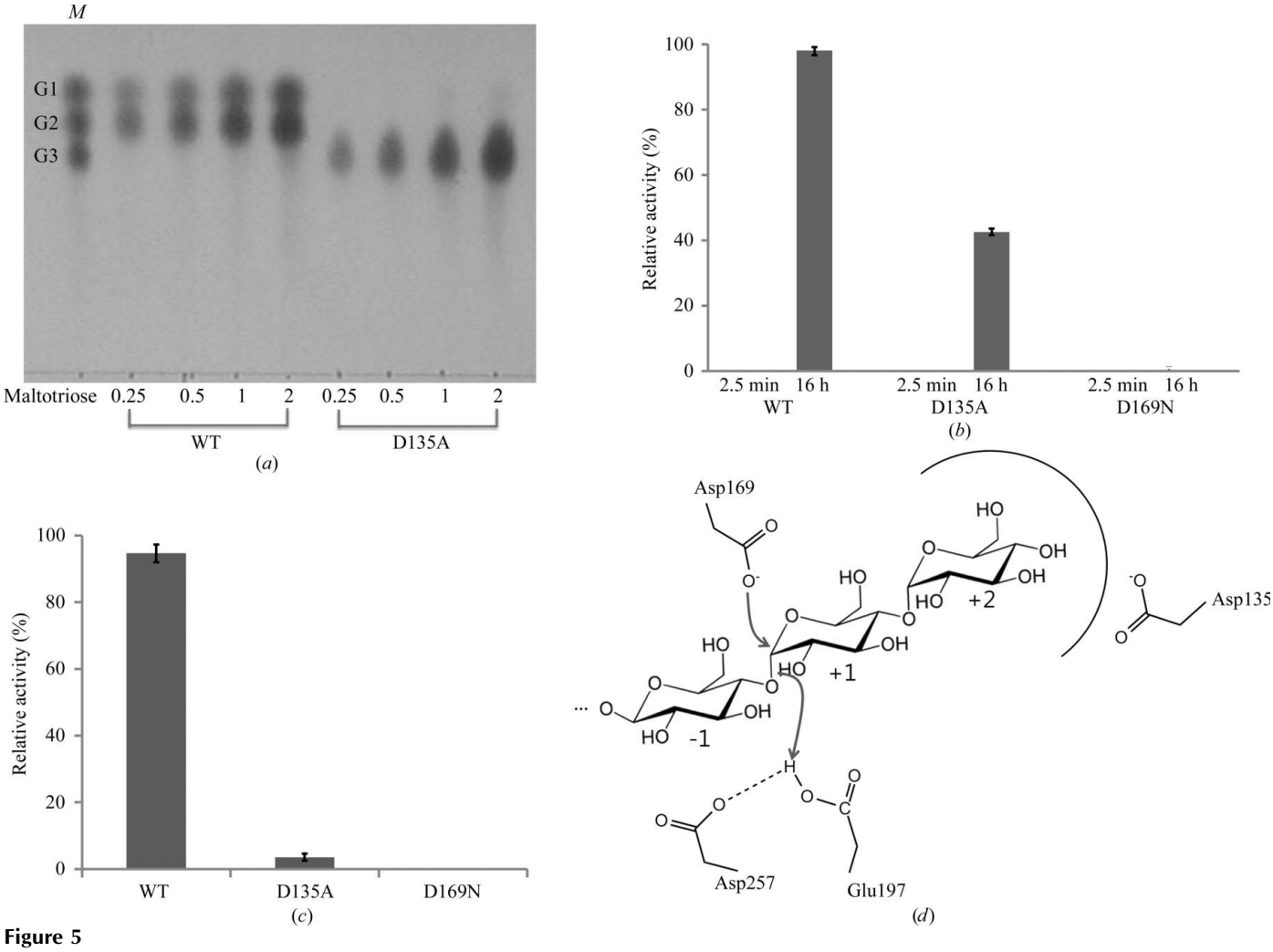

Figure 5
The role of Asp125 and the proposed mechanism of AmyB. (*a*) The D135A AmyB protein does not exhibit α-amylase activity in the α-amylase assay using maltotriose as a substrate. Increasing maltotriose (0.25, 0.5, 1 and 2%) was added to the enzyme solution containing wild-type (WT) or mutant (D135A) AmyB enzyme. Reaction mixtures were incubated at 348 K for 12 h and then subjected to TLC analysis. (*b*) The relative α-glucosidase activity of wild-type and mutant AmyB proteins using *p*-nitrophenyl glucopyranoside (pNPG) as a substrate. While no enzymatic activity was observed in 2.5 min, measurable activity was observed when the substrate was incubated for 16 h. The mutant (D135A) AmyB protein exhibits significant α-glucosidase activity in the pNPG-based assay compared with the wild-type enzyme (WT). A mutation at the catalytic residue (D169N) completely abolished the amylase activity. The error bars represent the standard deviation from three independent experiments. (*c*) The relative α-glucosidase activity of wild-type and mutant AmyB proteins using *p*-nitrophenyl maltopyranoside ($pNPG_2$) as a substrate. The substrate was incubated with the AmyB proteins for 2.5 min. The same amounts of the enzyme and substrate were employed as in (*b*). The error bars represent the standard deviation from three independent experiments. (*d*) A proposed mechanism for recognition of the substrate at the active site of AmyB. When the nonreducing end of the sugar (+2 site) is recognized by the nonreducing end binding site lined by Asp135, the +1 and −1 sites of the substrate are positioned at the active-site pocket containing the catalytic triad (Asp169, Glu197 and Asp257). The reaction is then initiated by nucleophilic attack of Asp169 at the C1 atom of glucose (+1 site).

We thank Mijeong Choi for constructing the mutant proteins. This work was supported by a grant from the Korea Research Foundation (NRF-2012-00005548) to N-CH. This study made use of beamline NW3A at the Photon Factory AR, Tsukuba, Japan.

References

Adams, P. D., Grosse-Kunstleve, R. W., Hung, L.-W., Ioerger, T. R., McCoy, A. J., Moriarty, N. W., Read, R. J., Sacchettini, J. C., Sauter, N. K. & Terwilliger, T. C. (2002). *Acta Cryst.* D**58**, 1948–1954.

Ballschmiter, M., Fütterer, O. & Liebl, W. (2006). *Appl. Environ. Microbiol.* **72**, 2206–2211.

Bibel, M., Brettl, C., Gosslar, U., Kriegshäuser, G. & Liebl, W. (1998). *FEMS Microbiol. Lett.* **158**, 9–15.

Bok, J.-D., Yernool, D. A. & Eveleigh, D. E. (1998). *Appl. Environ. Microbiol.* **64**, 4774–4781.

Bronnenmeier, K., Kern, A., Liebl, W. & Staudenbauer, W. L. (1995). *Appl. Environ. Microbiol.* **61**, 1399–1407.

Brzozowski, A. M., Lawson, D. M., Turkenburg, J. P., Bisgaard-Frantzen, H., Svendsen, A., Borchert, T. V., Dauter, Z., Wilson, K. S. & Davies, G. J. (2000). *Biochemistry*, **39**, 9099–9107.

Chhabra, S., Parker, K. N., Lam, D., Callen, W., Snead, M. A., Mathur, E. J., Short, J. M. & Kelly, R. M. (2001). *Methods Enzymol.* **330**, 224–238.

Chhabra, S. R., Shockley, K. R., Conners, S. B., Scott, K. L., Wolfinger, R. D. & Kelly, R. M. (2003). *J. Biol. Chem.* **278**, 7540–7552.

Chhabra, S. R., Shockley, K. R., Ward, D. E. & Kelly, R. M. (2002). *Appl. Environ. Microbiol.* **68**, 545–554.
Clarke, A. J. & Svensson, B. (1984). *Calsberg Res. Commun.* **49**, 559–566.
Conners, S. B., Montero, C. I., Comfort, D. A., Shockley, K. R., Johnson, M. R., Chhabra, S. R. & Kelly, R. M. (2005). *J. Bacteriol.* **187**, 7267–7282.
DeLano, W. (2002). *PyMOL*. http://www.pymol.org.
Duffaud, G. D., McCutchen, C. M., Leduc, P., Parker, K. N. & Kelly, R. M. (1997). *Appl. Environ. Microbiol.* **63**, 169–177.
Emsley, P. & Cowtan, K. (2004). *Acta Cryst.* D**60**, 2126–2132.
Janecek, S., Svensson, B. & Henrissat, B. (1997). *J. Mol. Evol.* **45**, 322–331.
Kim, I.-C., Cha, J.-H., Kim, J.-R., Jang, S.-Y., Seo, B.-C., Cheong, T.-K., Lee, D.-S., Choi, Y. D. & Park, K.-H. (1992). *J. Biol. Chem.* **267**, 22108–22114.
Kim, J.-S., Cha, S.-S., Kim, H.-J., Kim, T.-J., Ha, N.-C., Oh, S.-T., Cho, H.-S., Cho, M.-J., Kim, M.-J., Lee, H.-S., Kim, J.-W., Choi, K.-Y., Park, K.-H. & Oh, B.-H. (1999). *J. Biol. Chem.* **274**, 26279–26286.
Kim, Y.-M., Jeong, Y.-K., Wang, M.-H., Lee, W.-Y. & Rhee, H.-I. (2005). *Nutrition*, **21**, 756–761.
Kim, T.-J., Kim, M.-J., Kim, B.-C., Kim, J.-C., Cheong, T.-K., Kim, J.-W. & Park, K.-H. (1999). *Appl. Environ. Microbiol.* **65**, 1644–1651.
Landt, O., Grunert, H. P. & Hahn, U. (1990). *Gene*, **96**, 125–128.
Laskowski, R. A., Rullmann, J. A. C., MacArthur, M. W., Kaptein, R. & Thornton, J. M. (1996). *J. Biomol. NMR*, **8**, 477–486.
MacGregor, E. A., Janecek, S. & Svensson, B. (2001). *Biochim. Biophys. Acta*, **1546**, 1–20.
Matsuura, Y., Kusunoki, M., Date, W., Harada, S., Bando, S., Tanaka, N. & Kakudo, M. (1979). *J. Biochem.* **86**, 1773–1783.
Matsuura, Y., Kusunoki, M., Harada, W., Tanaka, N., Iga, Y., Yasuoka, N., Toda, H., Narita, K. & Kakudo, M. (1980). *J. Biochem.* **87**, 1555–1558.
McCarter, J. D. & Withers, S. G. (1994). *Curr. Opin. Struct. Biol.* **4**, 885–892.
Miller, E. S. Jr, Parker, K. N., Liebl, W., Lam, D., Callen, W., Snead, M. A., Mathur, E. J., Short, J. M. & Kelly, R. M. (2001). *Methods Enzymol.* **330**, 246–260.
Otwinowski, Z. & Minor, W. (1997). *Methods Enzymol.* **276**, 307–326.
Park, K.-M., Jun, S.-Y., Choi, K.-H., Park, K.-H., Park, C.-S. & Cha, J. (2010). *Appl. Microbiol. Biotechnol.* **86**, 555–566.
Park, K.-H., Kim, T.-J., Cheong, T.-K., Kim, J.-W., Oh, B.-H. & Svensson, B. (2000). *Biochim. Biophys. Acta*, **1478**, 165–185.
Parker, K. N., Chhabra, S. R., Lam, D., Callen, W., Duffaud, G. D., Snead, M. A., Short, J. M., Mathur, E. J. & Kelly, R. M. (2001). *Biotechnol. Bioeng.* **75**, 322–333.
Robyt, J. F. & Mukerjea, R. (1994). *Carbohydr. Res.* **251**, 187–202.
Saul, D. J., Williams, L. C., Reeves, R. A., Gibbs, M. D. & Bergquist, P. L. (1995). *Appl. Environ. Microbiol.* **61**, 4110–4113.
Svensson, B. (1994). *Plant Mol. Biol.* **25**, 141–157.
Thompson, J. D., Gibson, T. J., Plewniak, F., Jeanmougin, F. & Higgins, D. G. (1997). *Nucleic Acids Res.* **25**, 4876–4882.
Vagin, A. & Teplyakov, A. (2010). *Acta Cryst.* D**66**, 22–25.
Vujičić-Žagar, A. & Dijkstra, B. W. (2006). *Acta Cryst.* F**62**, 716–721.
Windberger, E., Huber, R., Trincone, A., Fricke, H. & Stetter, K. O. (1989). *Arch. Microbiol.* **151**, 506–512.